Antimony segregation in the oxidation of AlAsSb interlayers

A. M Andrews, K. L. van Horn, T. Mates, and J. S. Speck[a)]
Materials Department, University of California, Santa Barbara, California 93106

(Received 13 February 2003; accepted 4 August 2003; published 2 October 2003)

The lateral wet oxidation of strained AlAsSb was studied. $AlAs_{0.80}Sb_{0.20}$ interlayers were grown on a GaAs substrate and capped with a lattice-matched $In_{0.25}Ga_{0.75}As$ layer. The AlAsSb was oxidized between 350 and 450 °C. Oxidation temperatures >400 °C resulted in poor surface morphology and delamination. Oxidation of thicker AlAsSb interlayers ($h \approx 2000$ Å) resulted in metallic Sb layers forming between the AlO_x and the semiconductor interfaces. The remaining Sb metal at the oxide–semiconductor interface was ~15% oxidized. Lateral wet oxidation of thinner AlAsSb interlayers ($h \leqslant 500$ Å) resulted in Sb inclusions at the oxide–semiconductor interface. The Sb inclusions were 1.5–2.0 μm in diameter and the inclusion thickness was approximately equal to the AlAsSb layer thickness. Methanol (CH_3OH) was added to the water mixture with the intent to stabilize the otherwise unstable stibine (SbH_3) such that Sb could be removed from the oxidizing structure. However, methanol addition resulted in a decreased oxidation rate and a change in the Sb precipitate morphology. The Sb inclusions observed in pure water oxidation changed to a Sb finger-like morphology with increasing methanol concentration. The Sb fingers were 1.0–2.0 μm wide and as long as the oxidation depth. Oxidation of AlAsSb interlayers $h \leqslant 200$ Å were limited by the incorporation of Ga from the substrate and capping layer into the oxidation layer. Doping the oxidation AlAsSb interlayer 1×10^{18} cm^{-3} *n* type (Si or Te) did not result in any improvement in Sb segregation. © *2003 American Vacuum Society.* [DOI: 10.1116/1.1613954]

I. INTRODUCTION

Dallesasse *et al*. first discovered the lateral wet oxidation of III–V interlayers when they noted the anisotropy in the oxidation of $Al_xGa_{1-x}As$–AlAs–GaAs superlattices.[1] Mesa structures were produced by etching, exposing buried Al-rich III–V layers and the structure was oxidized at temperatures in the range of 300–500 °C in a H_2O–N_2 gas environment. Today the lateral oxidation of III–V interlayers is of crucial importance to the fabrication of high-efficiency devices on III–V substrates. Lateral oxidation has proved essential in high-efficiency vertical-cavity surface emitting lasers (VCSELs).[2,3] A combined optical and electrical aperture is created by partially oxidizing the epilayer, which reduces scattering losses from the pillar edges and improves lasing efficiency. Although lateral oxidation is of greatest importance to the VCSEL community, the oxidation of the underlying material below transistors enables oxide gate insulators and device isolation in III–V electronic devices.[4–7]

For lateral oxidation structures on GaAs substrates, the oxidation reaction in the AlAs interlayers is limited by the removal of the oxidation byproduct AsH_3.[8] The porous oxide provides a route for the diffusion of the reactants and byproducts. The formation of atomic hydrogen and the formation of AsH_3 limit the oxidation rate and the final oxide composition. The oxidation rate of AlAs shows a strong dependence on the layer thickness when $h \leqslant 500$ Å, where the thinner structures oxidize more slowly.[9] Linear oxidation rates are observed in thicker films between 400 and 500 °C, where the oxidation is reactant limited.

The transition to larger lattice parameter substrates requires a different oxidation interlayer in order to be lattice matched to the substrate. The available III–V oxide precursors between the lattice parameters of the GaAs (5.654 Å), InP (5.869 Å), InAs (6.058 Å), and GaSb (6.095 Å) substrates are variations of AlAs and alloys with Ga and In on the group III site and Sb on the group V site. During oxidation, the addition of only a few percent of Ga or In to the oxidation layer reduced the oxidation rate while the addition of Sb increases the oxidation rate.[10–15] The decreased oxidation rate in the Ga or In containing compounds requires an increase in oxidation temperature or time that is usually unacceptable for device processing.[13–15] Using the acceptable processing temperatures for InP, that leaves only one practical choice for an oxidation interlayer, $AlAs_{1-x}Sb_x$. The $AlAs_{1-x}Sb_x$ alloys oxidize between 300 and 450 °C, depending on alloy composition but result in an undesired byproduct of metallic Sb.[11] An AlAs interlayer shrinks ~20% after oxidation, but in the case of $AlAs_{1-x}Sb_x$, there is an overall swelling of the interlayer due to Sb segregation.[12] The oxidation of $AlAs_{1-x}Sb_x$ alloys result in Sb segregation to one of the oxide–semiconductor interfaces. Most reported experiments involved $AlAs_{1-x}Sb_x$ alloys lattice matched to InP substrates. In some cases, the Sb layer was reported to be at the upper interface,[12,16] while others reported Sb segregation to the lower interface.[17] Salesse reported that wet oxidation using water:methanol mixtures can suppress or eliminate the Sb segregation layer in *n*-type $AlAs_{0.56}Sb_{0.44}$ lattice matched to InP.[18] The same was not true for *p*-type $AlAs_{0.56}Sb_{0.44}$, while unintentionally doped epilayers were not investigated.

Seo *et al*. reported the first observation of strain relaxation by wet oxidation.[19] A schematic for a generic strain enhanced structure is shown in Fig. 1. The strain relaxation in the

a)Electronic mail: speck@mrl.ucsb.edu

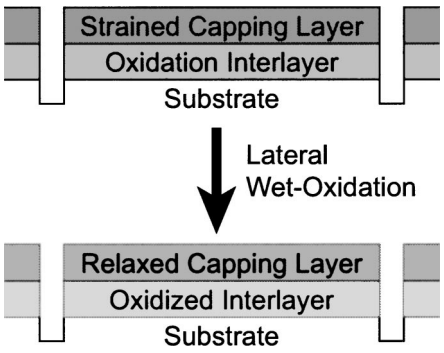

FIG. 1. Schematic of the relaxation enhanced structures before and after lateral wet oxidation. Mesas are produced by etching to expose the oxidation interlayer. The strained capping layer is partially relaxed after the interlayer is wet oxidized.

InGaAs/GaAs superlattice grown on an AlAs oxidation layer was found to increase with increasing indium composition or AlAs thickness. They concluded that a larger residual strain would result in a greater driving force for relaxation. Chavarkar *et al.* showed that the strain relaxation of $In_xGa_{1-x}As$ layers ($x=0.2$, 0.3, and 0.4) in $In_xGa_{1-x}As/AlAs/GaAs$ structures after oxidation depended greatly on the as-grown relaxation.[20] As the indium composition increased, so did the as-grown relaxation for the $h \approx 20h_c$ films, where h_c is the Matthews–Blakeslee critical thickness.[21] The critical thickness h_c is defined as the film thickness where it first becomes energetically favorable to introduce misfit dislocations at the film-substrate interface to relieve strain energy in the film, and as a result, the film thickness must be greater than h_c for relaxation to occur. The greater initial relaxation resulted in less strain relaxation after oxidation. Mathis *et al.* showed that the relaxation after lateral oxidation was due to the reduction of the misfit dislocation (MD) array line length at the InGaAs/AlAs interface by 2 orders of magnitude.[22] The threading dislocation (TD) density is relatively unchanged after oxidation. The removal of the MD cores reduced the energetic barrier to TD motion and thus relaxation. Films grown beyond the equilibrium critical thickness h_c show an additional strain relief of ~0.5% after lateral oxidation. Mathis also showed that the strain relaxation occurred at the oxidation front and not gradually over the oxidized layer.[22,23] Romanov *et al.* noted that the removal of the MD core correlates to an open core dislocation and the elastic fields are reduced on the order of the open core diameter, thus a more porous oxide would correlate to a lower energetic barrier to TD motion.[24] Therefore, the ideal structure for enhancing film relaxation would be a highly strained as-grown capping layer and the oxidation material and conditions that would form a highly porous oxide.

The goal of this study is to characterize and evaluate $AlAs_{1-x}Sb_x$ interlayers as a viable material for lateral wet oxidation interlayers in strained film relaxation and relaxation enhanced templates.

II. EXPERIMENT

Epitaxial $In_xGa_{1-x}As/AlAs_{1-x}Sb_x$ films were grown on GaAs (100) semi-insulating substrates by molecular beam epitaxy with cracked arsenic (As_2) and antimony (Sb_2) sources. For this study, lattice matched "analog alloys" of $In_{0.25}Ga_{0.75}As/AlAs_{0.80}Sb_{0.20}$ layers, which correspond to 1.8% lattice mismatch with the underlying GaAs substrate, were deposited at 500 °C. The Matthews–Blakeslee critical thickness for these films was $h_c \approx 50$ Å. The structures studied are in Table I, which are referred to as structures A–I. Each sample had the same lattice matched $In_{0.25}Ga_{0.75}As$ capping layer on an $AlAs_{0.80}Sb_{0.20}$ oxidation layer grown on a GaAs substrate. For these growth conditions and alloy compositions, a 250 Å layer ($5h_c$) was completely strained.

On-axis and off-axis high-resolution x-ray diffraction scans were performed on the (004), (115), and $(\bar{1}\bar{1}5)$ reflections to determine the layer composition and the extent of strain relaxation. The in-plane and relaxed lattice parameters were calculated from the substrate-layer peak separation using the technique in Ref. 25. The highly relaxed as-grown films were unsuitable for a study of enhanced relaxation from AlAsSb oxidation layers.

TABLE I. Samples used in this study were of the same $In_{0.25}Ga_{0.75}As/AlAs_{0.80}Sb_{0.20}$ composition grown at 500 °C on a GaAs substrate but with varying layer thickness and *n*-type doping.

Sample	*h* InGaAs (Å)	*h* AlAsSb (Å)	Doping (cm^{-3})	As grown ~% relaxed	Oxidized ~% relaxed
A	3000	2000	UID[a]	98	98
B	500	500	UID[a]	76	90
C	350	200	UID[a]	30	X[b]
D	300	200	UID[a]	0	X[b]
E	250	200	UID[a]	0	X[b]
F	200	200	UID[a]	0	X[b]
G	200	150	UID[a]	0	X[b]
H	500	500	Si (1×10^{18} cm^{-3})	80	90
I	500	500	Te (1×10^{18} cm^{-3})	80	90

[a]Unintentionally doped structures.
[b]Poor crystal quality in the capping layer for determining the film relaxation.

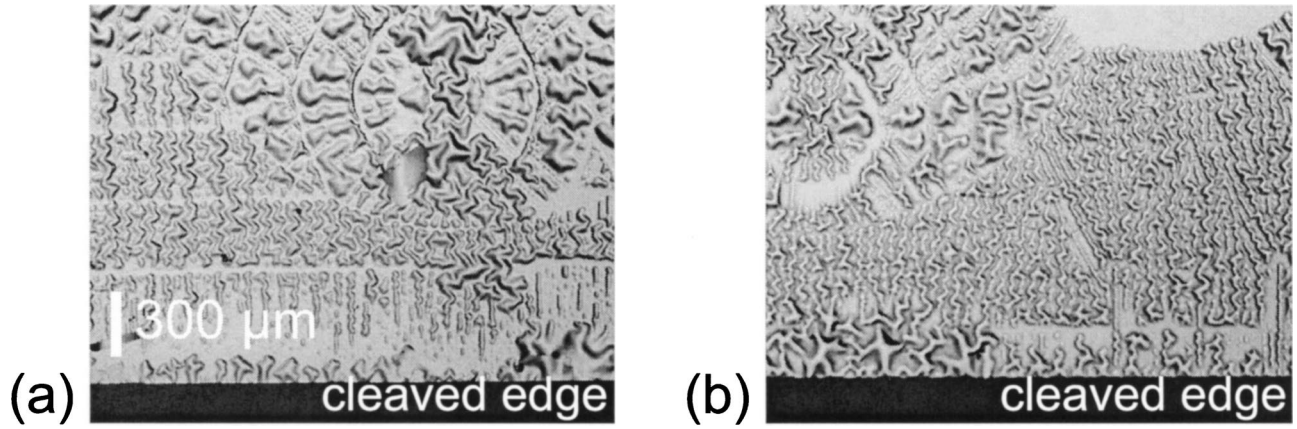

FIG. 2. Optical Nomarski micrographs of an oxidized cleaved edge of sample A at 450 °C. The water:methanol ratio during the wet oxidation was 1:0 in micrograph (a) and 1:3 in micrograph (b). The large variations in surface morphology are attributed to Sb segregation.

Etching 100-μm-square mesas and trenches exposed the oxidation layers. Reactive ion etching (RIE) of the mesas and trenches with Cl_2/Ar produced superior results to a $H_3PO_4:H_2O_2:H_2O$ wet etch. The Sb-containing layer was preferentially removed by the wet etch ($>$10:1) creating an undercut. The undercut became a stress concentration and resulted in delamination in most oxidation conditions. The RIE produced a less severe undercut and nearly eliminated the delamination.

The samples were wet oxidized in a furnace by bubbling nitrogen through a water:methanol solution at 70 °C. The oxidation was done at furnace temperatures between 350 and 450 °C with water:methanol mixtures of 1:0, 3:1, 1:1, 1:3, and 0:1. The films were characterized both before and after oxidation to evaluate the effects of the water:methanol mixture on the oxidation reactions. Following oxidation, the samples were optically photographed using a Nomarski interference microscope. The technique revealed large surface and subsurface features in the case of the thinner ($h \leqslant 500$ Å capping layer) samples. The average oxidation rates were determined by the known magnification of the Nomarski photographs.

The films were examined in cross-sectional high-resolution scanning electron microscopy (SEM). With the SEM, the Sb segregation, oxide shrinkage, and overall structure swelling were evident. The cross-sectional SEM samples were mounted with the surface oriented 70° to the incident electron beam and some surface features seen in Nomarski were evident. Atomic force microscopy (AFM) was used to determine the surface height profile and film roughness. Selective area secondary ion mass spectrometry (SIMS) and x-ray photoelectron spectroscopy (XPS) were used to determine the chemical composition as a function of depth in the oxidized layers. The SIMS and XPS were done to corroborate the images seen in the SEM. The SIMS data were collected with a Physical Electronics 6650 with an O_2^+ plasma source and a quadrupole detector. The XPS spectra was collected with a Kratos Axis Ultra with a 4 keV Ar gun, an $Al_{k\alpha}$ (1486 eV) x-ray source, and a 165 mm hemispherical detector.

III. RESULTS

A. Oxidation dependence on temperature

Samples A and B were oxidized at temperatures between 350 and 450 °C. The average oxidation rate of $AlAs_{0.80}Sb_{0.20}$ at temperatures below 350 °C was considered not sufficient for the lateral wet oxidation of the 100 μm mesas in 12 h. Lateral wet oxidation at temperatures above 400 °C resulted in extensive Sb segregation and frequent delamination of the mesa structures. Sample A was cleaved and then laterally wet oxidized at 450 °C. The raised features of the $In_{0.25}Ga_{0.75}As$ capping layer, seen in the Nomarski micrograph of sample A in Fig. 2, are attributed to the Sb segregation during the lateral wet oxidation of the $AlAs_{0.80}Sb_{0.20}$ interlayer. The extensive surface height variation makes temperatures $>$400 °C undesirable for future processing. The measured average oxidation rates at 400 °C of AlAs, $AlAs_{0.80}Sb_{0.20}$, and $AlAs_{0.56}Sb_{0.44}$ in pure water were 1.1, 2.0, and 4.5 μm/min.[12] The oxidation rates for samples A and B are plotted in Fig. 3. The oxidation rate scaling proportional to the interlayer thickness is negligible when the oxidation layer thickness h was greater than 500 Å.

B. Water:methanol oxidation

The AlAsSb interlayers oxidize rapidly at low oxidation temperatures compared to AlAs. Methanol was added to the wet oxidation water mixture in an attempt to provide more hydrogen free radicals to stabilize the SbH_3 so the byproduct could diffuse out of the mesa.[18] The introduction of methanol to the wet oxidation process reduced the oxidation rate. At 375 and 400 °C a water:methanol mixture of 1:3 reduced the wet oxidation rate to 50% of pure water and a pure methanol mixture did not oxidize at all. The oxidation front as well as the Sb inclusions and fingers can be seen in Fig. 4. At furnace temperatures of 350 °C and lower, the higher methanol fraction mixtures reduced the oxidation rate that is not practical for a 100 μm mesa. Lateral wet oxidation with

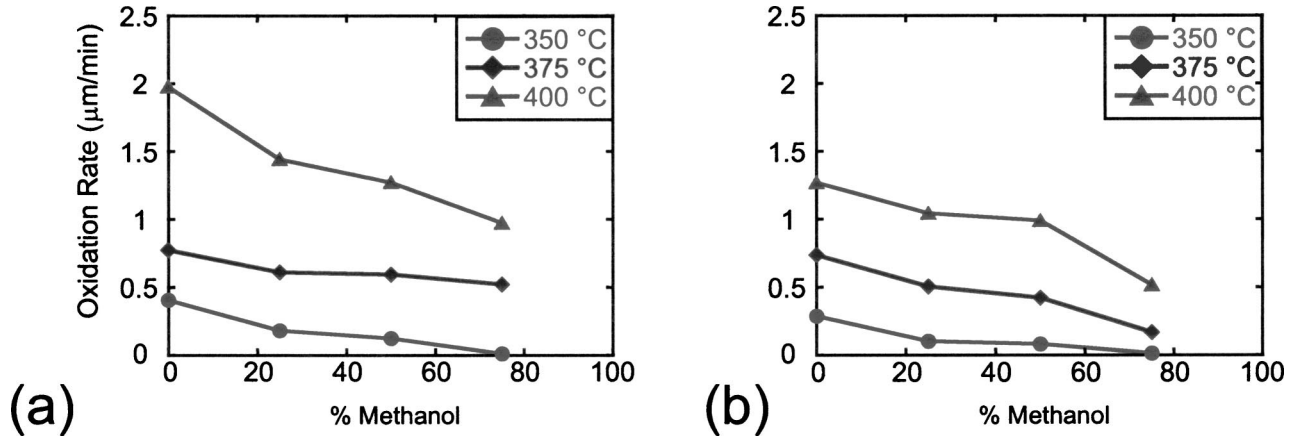

FIG. 3. Oxidation rates for $AlAs_{0.80}Sb_{0.20}$ interlayers. The average lateral wet oxidation rates for a 2000 Å $AlAs_{0.80}Sb_{0.20}$ interlayer are shown in (a) while the wet oxidation rates for a 500 Å interlayer are shown in (b). The increasing methanol concentration in the water:methanol mixture decreases the average lateral wet oxidation rate. Oxidation did not occur in pure methanol.

water:methanol mixtures also significantly reduced the delamination of the strained layer seen with pure water, which can be a side effect of the reduced oxidation rate.

AFM characterization of the surface of sample A showed an increase in surface roughness with increasing oxidation temperature. X-ray diffraction, after oxidation, showed little change in the relaxation of the $h = 3000$ Å $In_{0.25}Ga_{0.75}As$ layer, but this was expected due to the large extent of initial relaxation. There is more information about the laterally oxidized interlayer in the optical Nomarski micrographs of

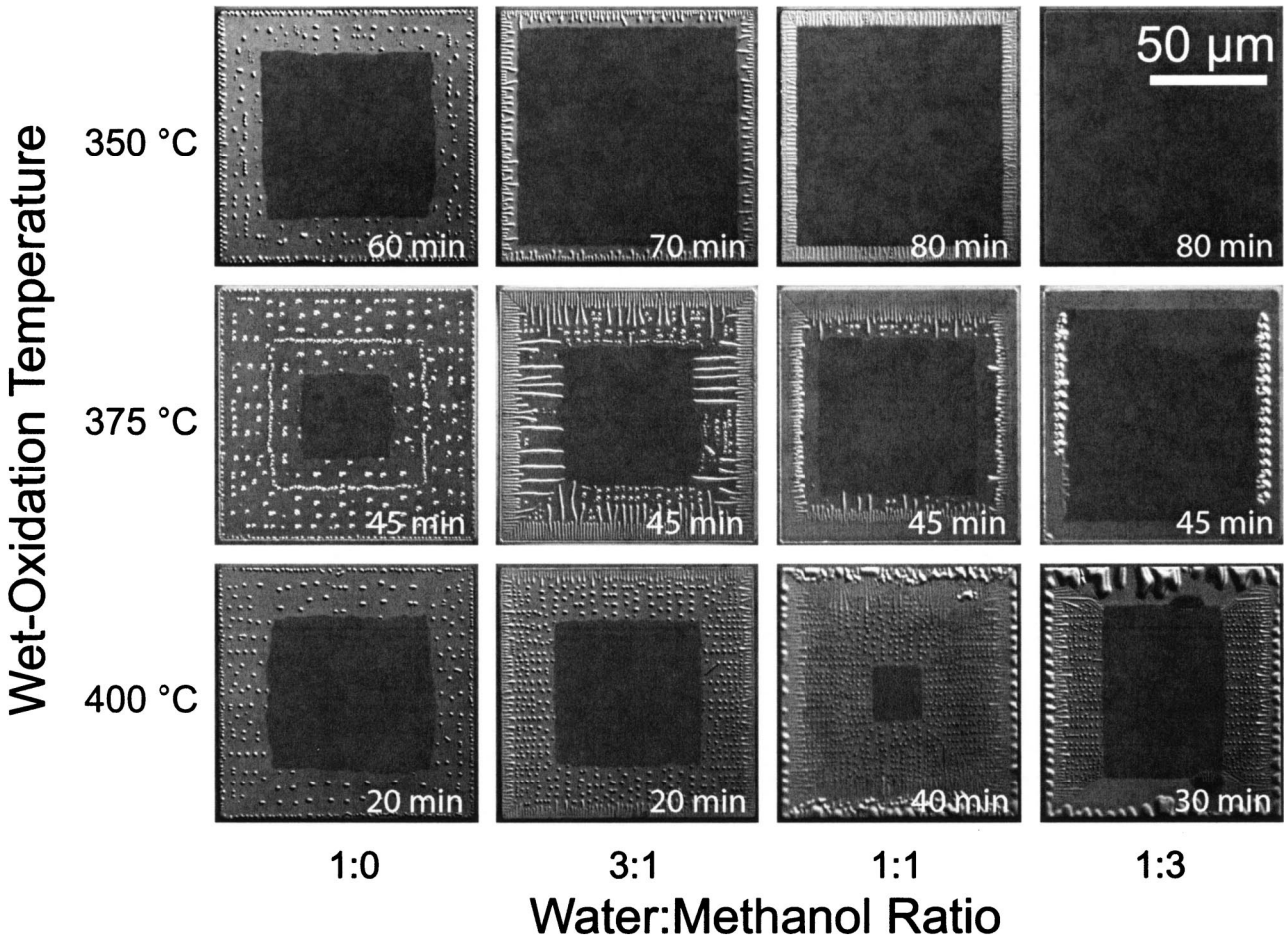

FIG. 4. Optical Nomarski micrographs of sample B after lateral wet oxidation. The oxidation temperatures are shown vs the ratio of water:methanol in the wet oxidation mixture. Increasing the wet oxidation temperature produced a rougher surface morphology. The increase of methanol in the water:methanol mixture reduced the average wet oxidation rate and at lower temperatures improved the surface morphology. The 1.5–2.0 μm diam inclusions turned to 1.5–2.0 μm wide fingers with the increasing methanol concentration.

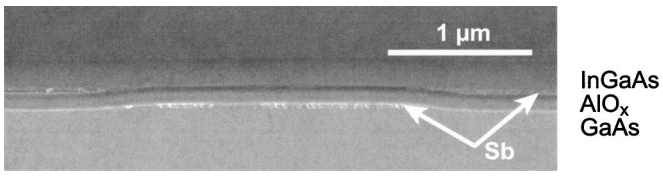

FIG. 5. Cross-sectional SEM of sample A wet oxidized at 375 °C with a solution of 3:1 water:methanol. Sb (bright layers in the micrograph) appears on both the top and bottom interface independent of oxidation temperature and water:methanol concentration.

sample B, shown in Fig. 4, due to the semitransparent $h = 500$ Å $In_{0.25}Ga_{0.75}As$ capping layer. The 1.5–2.0 μm diam inclusions seen in the micrograph resulted from Sb segregation and the inclusions were measured by AFM to be approximately the height of the oxidation interlayer thickness. With the increasing methanol concentration, the inclusions were observed as 1.0–2.0 μm wide fingers. The Sb inclusions and film delamination increased with oxidation temperature. The anisotropy between the two orthogonal $\langle 011 \rangle$ oxidation directions was more prevalent with the Sb segregation in the 375 °C 1:3 water:methanol oxidized sample. The Sb segregates into visible fingers only in the $[0\bar{1}1]$ direction and appears to neither blister nor form Sb fingers in the [011] direction.

C. Oxidation dependence on interlayer thickness

Cross-sectional SEM of sample A was performed to observe the oxidized AlAsSb interlayer, as shown in Fig. 5. The Sb segregation was seen at the upper interface, lower interface, or both, independent of oxidation temperature or water:methanol mixture. The segregation was observed concurrently at both interfaces or either at the upper or lower interface within the same oxidation layer. To confirm the presence of Sb at both interfaces, selective area SIMS depth profiles were measured on as-grown, oxidized with pure water, and oxidized with different water:methanol mixtures by a 100 μm$\times$100 μm trench with a 10% gate (i.e., chemical analysis was performed on $\sim$30 μm$\times$30 μm area in the 100 μm$\times$100 μm trench). Antimony from the oxidation layer segregated to both interfaces independent of the oxidation conditions, as shown in Fig. 6. XPS, in Fig. 7, showed that the remaining Sb was $\sim$15% oxidized.

The relatively constant ratio of Sb segregation to layer thickness implies that a sufficiently thin AlAsSb oxidation layer would lead to only a few monolayers of Sb at the oxide–semiconductor interface. Oxidation layers with a thickness $h \leqslant 200$ Å in principle should have 2 monolayers of Sb at the interface. However, the thinner AlAsSb oxidation layers form Sb inclusions instead of thin Sb layers. The analysis of structures B–I by SEM and XPS only showed the Sb at the upper interface. Oxidation of the thinner layers resulted in the average oxidation rate decreasing with time. For example, the average oxidation rate for a 3 h oxidation was 0.13 μm/h, while the average oxidation rate for a 12 h oxidation was 0.07 μm/h.

Examination by depth dependent XPS of an unoxidized region of sample F that had been at 375 °C for 12 h showed diffusion of Ga into the oxidation layer, as shown in Fig. 8(a) with the cross section of the Ga and Al profiles shown in Fig. 8(b). The presence of Ga in the AlAsSb layers can explain the slow oxidation rate. As in AlGaAs oxidation, the concentration of Ga greatly affects the oxidation rate.[1]

D. *n*-type doping affect on oxidation

To investigate the influence of *n*-type doping, as published by Salesse *et al.*,[18] on the oxidation of AlAsSb, the oxidation layers of samples H and I were doped with Si and Te to $\sim 1\times10^{18}$ cm^{-3}. The samples were grown with a semitransparent 500 Å $In_{0.25}Ga_{0.75}As$ cap to simplify the characterization of the effect of doping on Sb segregation. As seen in Fig. 9, there is no significant effect of *n*-type doping on the segregation of Sb. The Sb inclusions were observed in the oxidized interlayers. There was also little difference between the Te and Si *n*-type doping. For the oxidation of large lateral distances, as in the 100 μm mesas used, the *n*-type doping did not affect Sb segregation.

IV. DISCUSSION

This study was motivated by the need for high crystalline quality growth templates with lattice parameters not available from binary III–V substrates. Competing characteristics of a highly strained film before lateral wet oxidation and a large lattice parameter film limit the application of lateral wet oxidation for strain relaxation on GaAs substrates. The next largest lattice parameter III–V substrate after GaAs is InP. Due to processing time and temperature limitations, AlAsSb is the best alloy for an oxidation interlayer on InP but AlAsSb lateral wet oxidation results in Sb segregation at the oxide–semiconductor interface.

GaAs substrates were used for a starting lattice parameter and lattice matched $AlAs_{0.80}Sb_{0.20}$ and $In_{0.25}Ga_{0.75}As$ for the oxidation and capping layer. This is a strained oxidation and capping layer when most studies on AlAsSb oxidation were lattice matched to InP. The oxidation temperatures were limited between 350 and 450 °C. The average oxidation rates for lateral wet oxidation at temperatures below 350 °C were considered insufficient for the 100 μm mesas while lateral wet oxidation at temperatures above 400 °C resulted in large surface features attributed to the Sb segregation, at the oxide–semiconductor interface, and possible delamination of the mesas.

In oxidized sample A ($h = 2000$ Å), the Sb segregates from the AlO_x into a layer that is $\sim$85% Sb metal and $\sim$15% SbO_x, as shown in the XPS depth profiles in Fig. 7. This layer, as shown in Fig. 6, can be at the upper or lower oxide–semiconductor interface in the oxidized InGaAs/AlAsSb/GaAs structure. This Sb segregation layer resulted in a weak bond between the capping layer and oxide, which often resulted in the delamination of the InGaAs capping layer in subsequent film processing. The oxidation of samples B–I, $h \leqslant 500$ Å, resulted in the formation of Sb inclusions at the oxide–semiconductor interface instead of Sb layers. The Sb

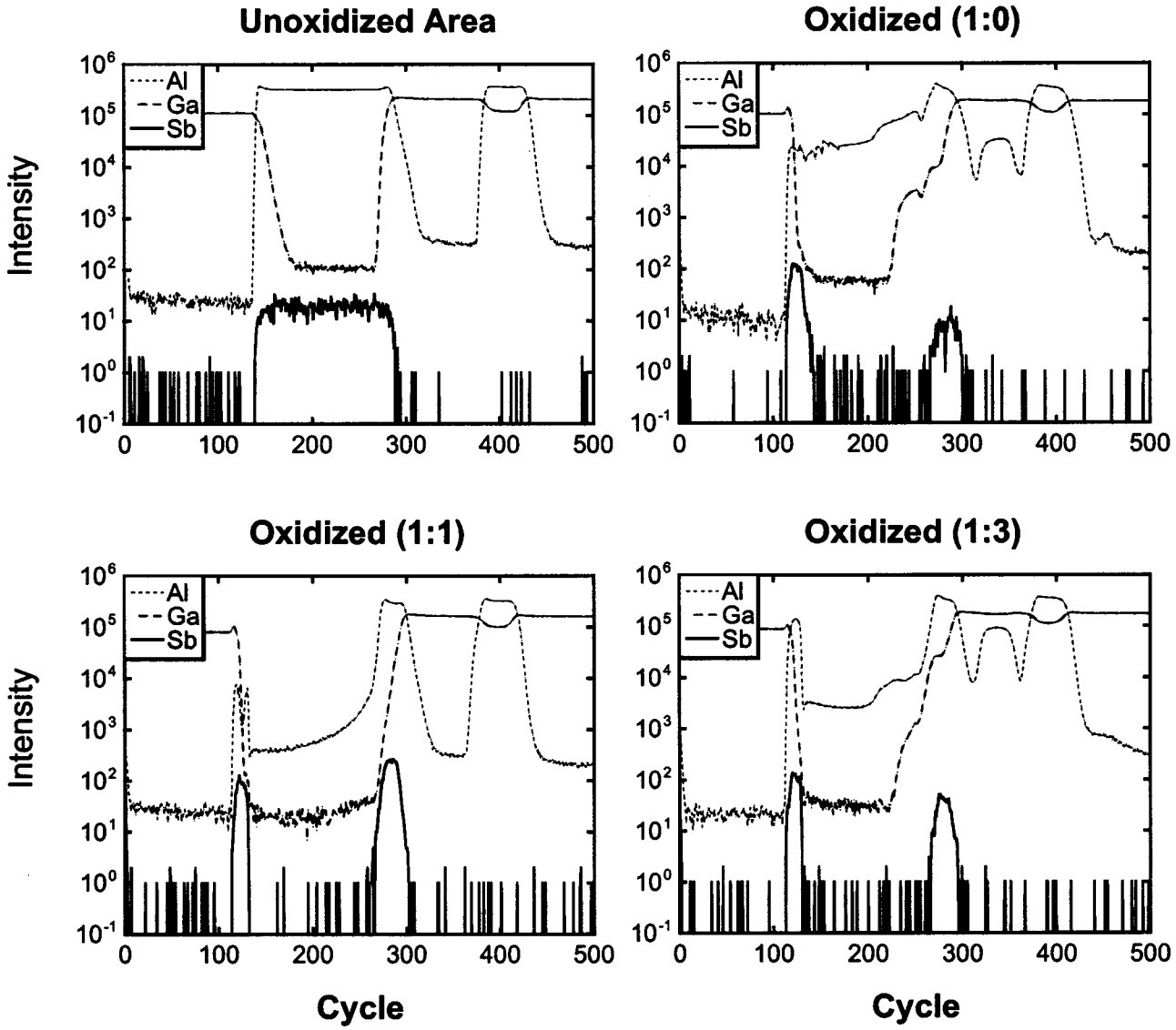

FIG. 6. SIMS depth profiles of sample A. After the oxidation of the AlAsSb interlayer, the Sb segregates to both the upper and lower oxide–semiconductor interfaces. The ratio of water:methanol during wet oxidation has little effect on the Sb segregation.

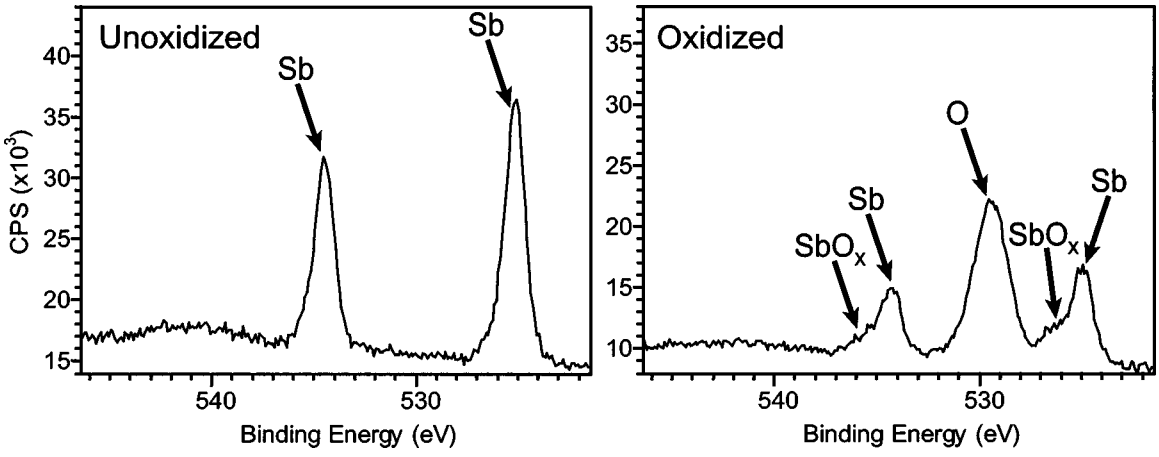

FIG. 7. XPS spectra of the $AlAs_{0.8}Sb_{0.2}$ interlayer before and after oxidation. The unoxidized spectrum shows the Sb in the AlAsSb interlayer. After lateral wet oxidation, the spectrum peaks corresponded to the remaining Sb that was 15% oxidized and the oxygen in the AlO_x interlayer.

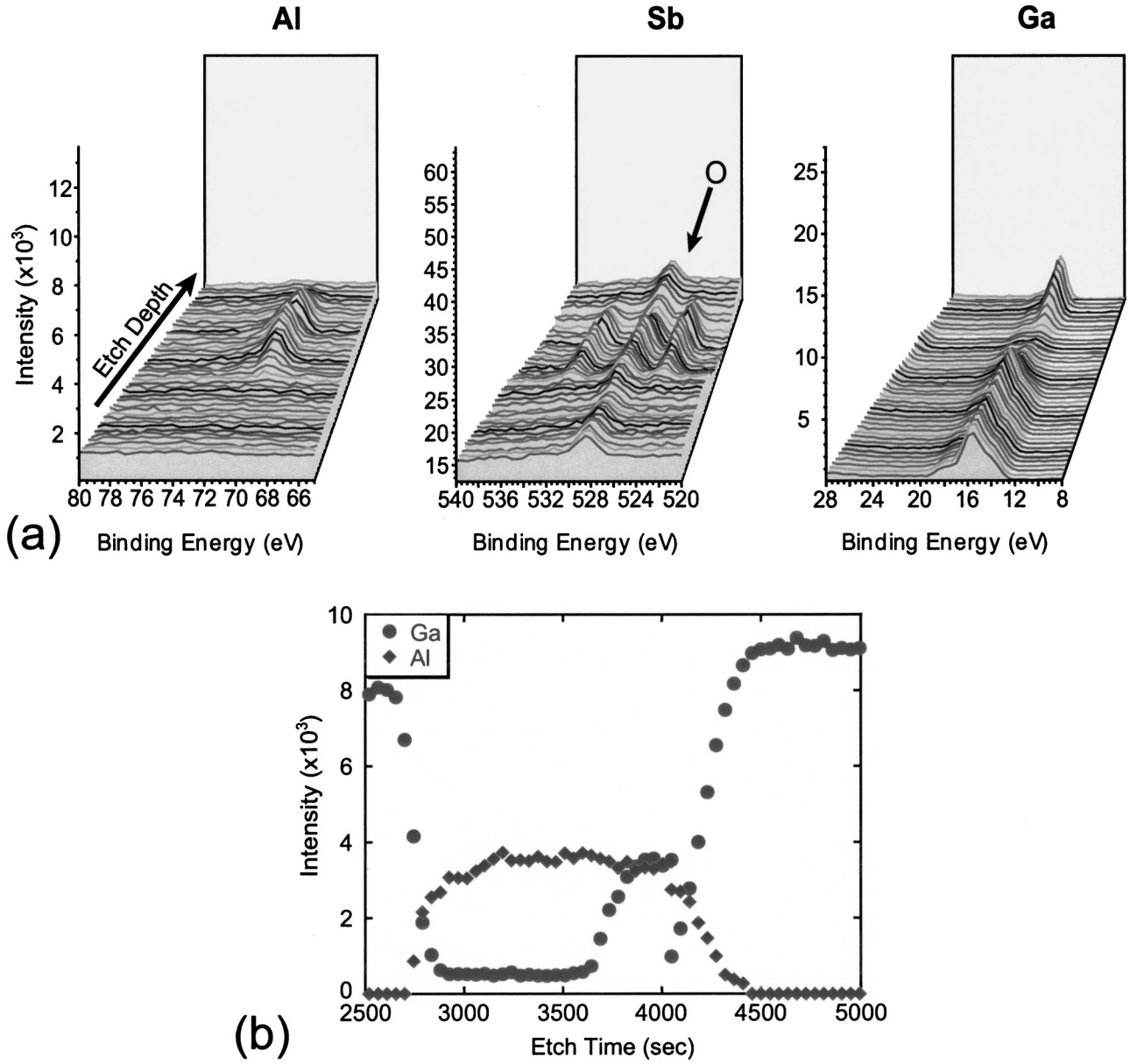

FIG. 8. X-ray photoelectron spectroscopy depth profiles of an unoxidized area of sample F annealed at 375 °C for 12 h. The InGaAs/AlAsSb/GaAs sample was Ar^+ etched between each scan. (a) The depth profiles of Al, Sb, and Ga are shown. (b) The plot of the Ga and Al peaks as a function of depth shows that the Ga has diffused into the AlAsSb layer from the GaAs substrate.

segregation did not disappear in the thinner samples but only reduced the number Sb of inclusions after lateral wet oxidation. Thicker capping layers may prevent the formation of Sb inclusions through the increased stiffness of thicker films, but that would defeat the purpose of growing a highly strained capping layer since thicker InGaAs capping layers would be relaxed. The oxidation rate becomes highly depressed when the AlAsSb thickness is $h<500$ Å. When the oxidation rate is slow enough, the diffusion of Ga into the AlAsSb interlayer from the surrounding layers further inhibits the AlAsSb oxidation.

The addition of an *n*-type dopant, Si or Te, to the AlAsSb interlayer at $\sim 1\times 10^{18}$ cm^{-3} did not affect the oxidation or the Sb segregation. The differences between the two different *n*-type dopants were negligible. It is possible that the surface charges, due to the dangling atomic bonds at the free surface, in the thinner structures B–I dominate the Sb migration and the doping of the oxidation layers is only useful in thicker structures where the oxidation layer is isolated from the surface charges.

Efficient electronic devices such as high electron mobility transistors should not have parallel conduction or current leakage paths. The formation of a metallic Sb layer between the oxide and the strain relaxed semiconducting layers thwarts any subsequent device fabrication. A thick insulating buffer layer would have to be grown on the relaxed capping layer in order to isolate the device and that would be counterproductive to the purpose of starting with a growth template. The growth template is supposed to be an epitaxy-ready substrate without a backside Schottky contact.

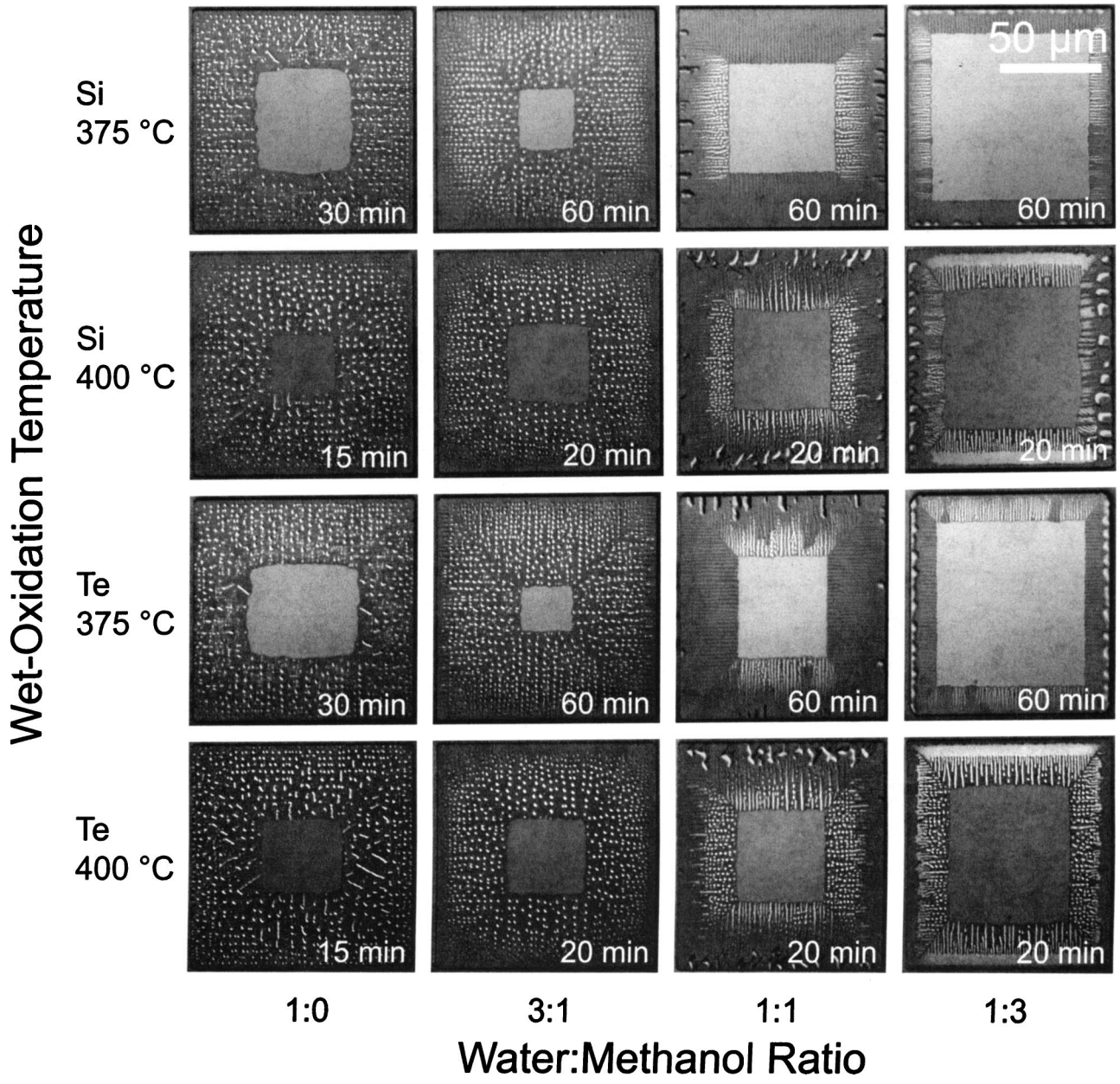

FIG. 9. Optical Nomarski micrographs *n*-type $AlAs_{0.80}Sb_{0.20}$ after oxidation. The oxidation temperatures and dopant species, Si and Te, are shown vs the ratio of water:methanol in the wet oxidation mixture. There is little effect of *n*-type doping to prevent the Sb segregation and inclusion formation during the oxidation of AlAsSb with or without methanol.

However, the oxidation of AlAsSb has been used in VCSEL technology to successfully form current and optical apertures.[26] The Sb precipitates present less of a problem with the optoelectronic devices when the current path is perpendicular to the oxidation layer and the precipitates are not contacted by either the *n*- or *p*-type ohmic metals.

V. SUMMARY

AlAsSb interlayers were laterally wet oxidized to enhance strain relaxation of misfitting layers. Different water:methanol environments were used to hinder the segregation of Sb at the oxide–semiconductor interfaces. Low lattice mismatch $AlAs_{0.80}Sb_{0.20}$ interlayers were grown on GaAs substrates to evaluate the oxidation. Lateral wet oxidation of AlAsSb interlayers at temperatures above 400 °C resulted in extensive Sb precipitation and delamination of the 100 μm mesas. Average lateral wet oxidation rates at temperatures below 350 °C were insufficient for the oxidation of the 100 μm mesas in 12 h. After lateral wet oxidation, the thicker $h = 2000$ Å $AlAs_{0.80}Sb_{0.20}$ interlayers formed an Sb layer at the oxide–semiconductor interface that was ~15% oxidized. The Sb layers can form at either oxide–semiconductor interface and seem to be independent of the lateral wet oxidation conditions. The lateral wet oxidation of the thinner $h \leqslant 500$ Å $AlAs_{0.80}Sb_{0.20}$ interlayers resulted in Sb inclusions forming blisters in the capping layer. The addition of metha-

nol to the wet oxidation mixture, to increase the available hydrogen free radicals and help stabilize the oxidation byproduct SbH_3, only seemed to decrease the average wet-oxidation rate. The decreased average wet oxidation rate of the $AlAs_{0.80}Sb_{0.20}$ interlayers coincided with a change in the segregated Sb morphology from inclusions to fingers. The *n*-type doping ($1\times10^{18}\,cm^{-3}$) with Si or Te of the $AlAs_{0.80}Sb_{0.20}$ interlayers did not suppress or result in any real change in the Sb precipitate morphology after lateral wet oxidation.

ACKNOWLEDGMENTS

This work made use of MRL Central Facilities supported by the National Science Foundation under Award No. DMR00-80034. This work was also supported by DARPA and AFOSR (W. Coblenz and G. Witt program managers).

[1]J. M. Dallesasse, N. Holonyak, Jr., A. R. Sugg, T. A. Richard, and N. El-Zein, Appl. Phys. Lett. **57**, 2844 (1990).
[2]N. Ohnoki, N. Hatori, A. Mizutani, F. Koyama, and K. Iga, J. Cryst. Growth **195**, 603 (1998).
[3]E. C. Vail, G. S. Li, W. Yuen, and C. J. Chang-Hasnain, Electron. Lett. **32**, 1888 (1996).
[4]A. C. Alonzo, X.-C. Cheng, and T. C. McGill, J. Appl. Phys. **84**, 6901 (1998).
[5]B.-K. Jun, D.-H. Kim, J.-Y. Leem, J.-H. Lee, and Y.-H. Lee, Thin Solid Films **360**, 229 (2000).
[6]H. Gebretsadik, K. Zhang, K. Kamath, X. Zhang, and P. Bhattacharya, Appl. Phys. Lett. **71**, 3865 (1997).
[7]E. I. Chen, N. Holonyak, Jr., and S. A. Maranowski, Appl. Phys. Lett. **66**, 2688 (1995).
[8]C. H. Ashby, J. P. Sullivan, K. D. Choquette, K. M. Geib, and H. Q. Hou, J. Appl. Phys. **82**, 3134 (1997).
[9]R. L. Naone and L. A. Coldren, J. Appl. Phys. **82**, 2277 (1997).
[10]P. Chavarkar, U. K. Mishra, S. K. Mathis, and J. S. Speck, Appl. Phys. Lett. **76**, 1291 (2000).
[11]O. Blum, M. J. Hafich, J. F. Klem, K. Baucom, and A. Allerman, Electron. Lett. **33**, 1097 (1997).
[12]S. K. Mathis, K. H. Lau, A. M. Andrews, E. M. Hall, G. Almuneau, E. L. Hu, and J. S. Speck, J. Appl. Phys. **89**, 2458 (2001).
[13]G. W. Pickrell, J. H. Epple, K. L. Chang, K. C. Hsieh, and K. Y. Cheng, Appl. Phys. Lett. **76**, 2544 (2000).
[14]J. P. Loehr and S. A. Feld, Proc. IEEE **2**, 110 (1998).
[15]B. Koley, F. G. Johnson, O. King, S. S. Saini, and M. Dagenais, Appl. Phys. Lett. **75**, 1264 (1999).
[16]O. Blum, K. M. Geib, M. J. Hafich, J. F. Klem, and C. I. H. Ashby, Appl. Phys. Lett. **68**, 3129 (1996).
[17]P. Legay, P. Petit, G. Le Roux, A. Kohl, I. F. L. Dias, M. Juhel, and M. Quillec, J. Appl. Phys. **81**, 7600 (1997).
[18]A. Salesse *et al.*, Appl. Surf. Sci. **161**, 426 (2000).
[19]J. H. Seo and K. S. Seo, Appl. Phys. Lett. **72**, 1466 (1998).
[20]P. Chavarkar, L. Zhao, S. Keller, A. Fisher, C. Zheng, J. S. Speck, and U. K. Mishra, Appl. Phys. Lett. **75**, 2253 (1999).
[21]J. W. Matthews and A. E. Blakeslee, J. Cryst. Growth **27**, 118 (1974).
[22]S. K. Mathis, P. Chavarkar, A. M. Andrews, U. K. Mishra, and J. S. Speck, J. Vac. Sci. Technol. B **18**, 2066 (2000).
[23]S. K. Mathis, A. M. Andrews, P. Chavarkar, U. K. Mishra, E. L. Hu, and J. S. Speck, Presented at Electronic Materials Conference, Denver, CO, 2000.
[24]A. E. Romanov and J. S. Speck, J. Electron. Mater. **29**, 901 (2000).
[25]A. Krost, G. Bauer, and J. Woitok, in *Optical Characterization of Epitaxial Semiconductor Layers*, edited by G. Bauer and W. Richter (Springer, New York, 1996), p. 287.
[26]M. H. M. Reddy, D. A. Buell, A. S. Huntington, T. Asano, R. Koda, D. Feezell, D. Lofgreen, and L. A. Coldren, Appl. Phys. Lett. **82**, 1329 (2003).